

# Propagation of Two-Photon Zernike States in Atmospheric Turbulence

Hakob Avetisyan

*Alikhanyan National Laboratory (Yerevan Physics Institute),  
2 Alikhanyan Brothers Street, Yerevan 0036, Armenia\**

Vahagn Abgaryan

*Alikhanyan National Laboratory (Yerevan Physics Institute),  
2 Alikhanyan Brothers Street, Yerevan 0036, Armenia and  
Joint Institute for Nuclear Research, 6 Joliot-Curie St., Dubna, 141980, Russia†*

We analyze propagation and detection of two-photon states expanded in Zernike modes through atmospheric turbulence using the extended Huygens–Fresnel formalism. For SPDC states prepared with a single Zernike pump mode, we analytically reduce the 8-dimensional continuous propagation integrals to an exact, discrete modal expansion. In the absence of turbulence, Zernike addition enforces conservation of azimuthal index and a strict radial-order bound. Turbulence relaxes these constraints, driving structured azimuthal and radial crosstalk dominated by low-order aberration modes. By explicitly removing the lowest-order terms from the discrete turbulence sum, we demonstrate that partial adaptive optics correcting only up to the sixth radial order is sufficient to heavily suppress this crosstalk and restore near-ideal spatial correlations.

## I. INTRODUCTION

Spatially structured optical fields provide a high-dimensional resource for quantum optics and quantum information processing, enabling enhanced encoding capacity, robustness, and sensitivity in tasks ranging from quantum communication to quantum sensing [1–8]. In particular, the transverse spatial degrees of freedom of photons generated via spontaneous parametric down-conversion (SPDC) can exhibit strong correlations and entanglement, which have been extensively studied using Hermite–Gaussian (HG) and Laguerre–Gaussian (LG) mode bases [9, 10]. These modal representations have played a central role in establishing conservation laws, selection rules, and entanglement properties of quantum states of spatially structured light.

In practical free-space implementations, however, spatially encoded quantum states must propagate through random or turbulent media, most notably the atmosphere. Atmospheric turbulence introduces random phase distortions that couple transverse modes, degrade modal orthogonality, and weaken spatial correlations. This manifests as severe intermodal crosstalk—most notably observed as the degradation of orbital angular momentum (OAM) selection rules—effectively acting as a noisy quantum channel [11–18]. Understanding how turbulence affects different spatial encodings is therefore a central problem in the development of robust quantum photonic technologies.

Turbulence-induced degradation of spatial correlations has been extensively investigated in HG and LG modal bases, frequently, within the extended Huygens–Fresnel formalism [19, 20]. However, both, the robustness of correlations and the structure of intermodal coupling depend

strongly on the chosen representation. In this work, we retain the same propagation framework while reformulating the analysis in the Zernike basis.

Motivated by this observation, we recently introduced Zernike polynomials as a physically meaningful basis for describing quantum states of light [21]. They are widely used in classical optics to represent wavefront aberrations, with low-order polynomials corresponding directly to familiar distortions such as piston, tilt, defocus, astigmatism, coma, and trefoil [22–24]. In the quantum context, we showed that SPDC can generate entanglement in the Zernike basis and that the associated expansion coefficients obey exact selection rules closely analogous to angular-momentum conservation in LG modes, while simultaneously encoding radial-order constraints absent in conventional OAM descriptions.

The direct correspondence between Zernike modes and classical aberrations suggests that this basis may offer distinct advantages for analyzing and mitigating turbulence-induced decoherence. Since atmospheric turbulence is itself commonly described in terms of low-order aberrations, one may expect that its dominant effects are naturally captured by a restricted subset of Zernike modes.

In this work, we develop a theoretical framework for the propagation and detection of Zernike-mode two-photon states through atmospheric turbulence. Using the extended Huygens–Fresnel principle, we incorporate random phase distortions into the Zernike-mode representation of the optical field and derive analytical expressions for the joint two-photon detection probability in the far field. The formalism allows us to separate the roles of state preparation, modal structure, and turbulence-induced mode coupling in a transparent and systematic manner.

Applying the theory to entangled photon pairs generated via SPDC, we analyze how turbulence modifies the exact selection rules that hold in the absence of random

\* h.avetisyan@yerphi.am

† vahagnab@googlemail.com

media. We show that while turbulence relaxes these constraints, the resulting degradation of spatial correlations is dominated by a small set of low-order Zernike modes associated with classical aberrations. This hierarchical coupling behavior contrasts with the extensive mode coupling observed in LG- and HG-based descriptions and provides a clear physical interpretation of turbulence-induced decoherence in terms of aberration dynamics.

In the present work, we adopt the same propagation framework but reformulate it in the Zernike basis, which is naturally adapted to aberration-driven distortions and allows the turbulence-induced coupling structure to be analyzed in a physically transparent manner. In addition to their application to quantum field propagation in turbulence, the Zernike and Fourier–Zernike coupling identities derived here provide a closed algebraic framework that may be useful in other contexts involving aberration-driven mode coupling.

The paper is organized as follows. Sec. II introduces the Zernike-mode formalism used throughout the work. In Sec. II A summarizes the properties of Zernike polynomials, their Fourier transforms, and the associated algebraic identities (some of which are new, to the best of our knowledge) required for two-photon mode coupling. Sec. II B and II C incorporate atmospheric turbulence into the Zernike-mode representation of the optical field operators using the extended Huygens–Fresnel principle. In Sec. III, we apply the formalism to the propagation and detection of entangled photon pairs generated via SPDC and derive analytical expressions for joint two-photon detection probabilities in atmospheric turbulence channel. Section IV discusses the physical implications of the results. Section V summarizes the main conclusions and outlines directions for future work.

## II. ZERNIKE-MODE FORMALISM AND FIELD PROPAGATION THROUGH TURBULENCE.

### A. Zernike modes and mode-coupling identities.

This subsection summarizes the Zernike and Fourier–Zernike identities required for subsequent derivations. Zernike modes form a complete orthonormal basis on the unit disk and provide a natural representation for optical fields defined on a circular pupil.

Unlike LG modes, Zernike modes impose explicit radial-order constraints. They are defined for integers  $m, n$  with  $n - |m| \geq 0$  and even as

$$Z_n^m(\boldsymbol{\rho}) = \begin{cases} \sqrt{n+1} R_n^{|m|}(\rho) e^{im\theta}, & 0 \leq \rho \leq 1, \\ 0 & \rho > 1, \end{cases} \quad (1)$$

where  $\boldsymbol{\rho} = (\rho, \theta)$ ,  $0 \leq \theta < 2\pi$ , are the polar coordinates ( $\rho = \sqrt{x^2 + y^2}$ ,  $\theta = \arctan(y/x)$ ), and the radial poly-

nomials  $R_n^{|m|}$  are given by

$$R_n^{|m|}(\rho, \theta) = \sum_{k=0}^{\frac{n-|m|}{2}} \frac{(-1)^k (n-k)!}{k! \left(\frac{n+m}{2} - k\right)! \left(\frac{n-m}{2} - k\right)!} \rho^{n-2k}. \quad (2)$$

We adopt the Fourier-transform convention

$$\tilde{f}(\mathbf{k}) = \int d^2\rho f(\mathbf{r}) e^{2\pi i \mathbf{r} \cdot \mathbf{k}}, \quad (3)$$

under which the Fourier transforms of Zernike modes exhibit a simple Bessel representation [22]

$$\begin{aligned} \tilde{Z}_n^m(\mathbf{q}) &= \int_0^1 d\rho \rho \int_0^{2\pi} d\theta Z_n^m(\rho, \theta) e^{2\pi i \rho q \cos(\theta - \phi)} \\ &= 2\pi i^n \sqrt{n+1} \frac{J_{n+1}(2\pi q)}{2\pi q} e^{im\phi}, \end{aligned} \quad (4)$$

where  $\mathbf{q} = (q, \phi)$  are polar coordinates in Fourier space.

The Zernike modes and their Fourier counterparts satisfy orthogonality and completeness relations. In real space (pupil plane), they are

$$\int d^2s Z_n^m(\mathbf{s}) Z_{n'}^{m'*}(\mathbf{s}) = \pi \delta_{nn'} \delta_{mm'}, \quad (5)$$

$$\sum_{n,m} Z_n^m(\mathbf{s}_1) Z_n^{m'*}(\mathbf{s}) = \pi \delta_D(\mathbf{s}_1 - \mathbf{s}). \quad (6)$$

where  $\delta_D(\mathbf{s}_1 - \mathbf{s}) = \mathbb{1}_D(\mathbf{s}_1) \mathbb{1}_D(\mathbf{s}_2) \delta(\mathbf{s}_1 - \mathbf{s}_2)$  is the delta function defined as the kernel of the projection onto the functions supported on a subset of the unit disk  $D$ .  $\mathbb{1}_D(\mathbf{s})$  denotes the indicator function of  $D$ , i.e.,  $\mathbb{1}_D(\mathbf{s}) = 1$  for  $\mathbf{s} \in D$ ,  $\mathbb{1}_D(\mathbf{s}) = 0$  otherwise. The analogous expressions for the Fourier space (image plane) are

$$\int d^2q \tilde{Z}_n^m(\mathbf{q}) \tilde{Z}_{n'}^{m'*}(\mathbf{q}) = \pi \delta_{nn'} \delta_{mm'}, \quad (7)$$

$$\begin{aligned} \sum_{n,m} \tilde{Z}_n^m(\mathbf{q}_1) \tilde{Z}_n^{m'*}(\mathbf{q}) &= \pi \frac{J_1(2\pi|\mathbf{q} - \mathbf{q}_1|)}{|\mathbf{q} - \mathbf{q}_1|} \\ &= \pi \tilde{Z}_0^0(\mathbf{q} - \mathbf{q}_1). \end{aligned} \quad (8)$$

The right-hand side of Eq. (8) is the integral kernel for the projector onto the subspace of  $\mathcal{F}\{L_D^2\} \subset L_{\mathbb{R}^2}^2$  i.e. functions with Fourier pre-image supported on the unit disk. Furthermore, the natural action of the projector on its eigenspace is guaranteed by the obvious relation

$$\int d^2q_1 \tilde{Z}_0^0(\mathbf{q} - \mathbf{q}_1) \tilde{Z}_n^m(\mathbf{q}_1) = \pi \tilde{Z}_n^m(\mathbf{q}). \quad (9)$$

These properties ensure a complete modal description of pupil- and image-plane optical fields. All projector identities below (including the kernels  $\delta_D$  and  $\tilde{Z}_0^0$ ) are to be understood only under integration against admissible test functions in the corresponding subspace.

Mode coupling in the Zernike basis is governed by two complementary sets of coefficients. The first are the  $A$ -coefficients, defined by the triple overlap integral [25]

$$A_{n_1 n_2 N}^{m_1 m_2 M} = \frac{1}{\pi} \int d^2s Z_{n_1}^{m_1}(\mathbf{s}) Z_{n_2}^{m_2}(\mathbf{s}) Z_N^{M*}(\mathbf{s}), \quad (10)$$

which encode exact Zernike-mode addition rules via Clebsch-Gordan (CG) coefficients (see Appendix A 1). This is equivalent to

$$Z_{n_1}^{m_1}(\mathbf{s}) Z_{n_2}^{m_2}(\mathbf{s}) = \sum_{NM} A_{n_1 n_2 N}^{m_1 m_2 M} Z_N^M(\mathbf{s}). \quad (11)$$

From the definition (10) there follow additional identities (see Appendix A for derivations),

$$\sum_{\substack{n_1, m_1 \\ n_2, m_2}} A_{n_1 n_2 N}^{m_1 m_2 M} Z_{n_1}^{m_1}(\mathbf{s}_1) Z_{n_2}^{m_2}(\mathbf{s}_2) = \pi Z_N^M(\mathbf{s}_1) \delta_D(\mathbf{s}_1 - \mathbf{s}_2), \quad (12)$$

$$\sum_{\substack{n_1, m_1 \\ n_2, m_2}} A_{n_1 n_2 N}^{m_1 m_2 M} \tilde{Z}_{n_1}^{m_1}(\mathbf{q}_1) \tilde{Z}_{n_2}^{m_2}(\mathbf{q}_2) = \pi \tilde{Z}_N^M(\mathbf{q}_1 + \mathbf{q}_2). \quad (13)$$

A second set of coefficients, denoted  $\Gamma$ , arises from convolution and linearization of Zernike modes. The corresponding real-space identity, for  $0 \leq |\mathbf{s}| \leq 2$ , [26, 27]

$$(Z_n^m * Z_{n'}^{m'}) (\mathbf{s}) = \sum_{n''m''} \Gamma_{nn'n''}^{mm'm''} Z_{n''}^{m''}(\mathbf{s}/2), \quad (14)$$

and its obvious implication, the linearization of Fourier-Zernike modes,

$$\tilde{Z}_n^m(\mathbf{q}) \tilde{Z}_{n'}^{m'}(\mathbf{q}) = 4 \sum_{n''m''} \Gamma_{nn'n''}^{mm'm''} \tilde{Z}_{n''}^{m''}(2\mathbf{q}), \quad (15)$$

which follows from applying the convolution theorem to Eq. (14). (notice, Eq. (14) slightly differs from that of Refs. [26, 27] – the second function in the convolution is not conjugated here.) Hence, the definition of the coefficients  $\Gamma$  can be taken as

$$\Gamma_{nn'n''}^{mm'm''} = \frac{1}{\pi} \int d^2q \tilde{Z}_n^m(\mathbf{q}) \tilde{Z}_{n'}^{m'}(\mathbf{q}) \tilde{Z}_{n''}^{m''*}(2\mathbf{q}). \quad (16)$$

From (16) also follows (see Appendix A)

$$\sum_{\substack{n_1, m_1 \\ n_2, m_2}} \Gamma_{n_1 n_2 N}^{m_1 m_2 M} \tilde{Z}_{n_1}^{m_1*}(\mathbf{q}_1) \tilde{Z}_{n_2}^{m_2*}(\mathbf{q}_2) = \pi \int d^2q \tilde{Z}_N^{M*}(2\mathbf{q}) \tilde{Z}_0^0(\mathbf{q} - \mathbf{q}_1) \tilde{Z}_0^0(\mathbf{q} - \mathbf{q}_2), \quad (17)$$

and double inverse Fourier transforming, we get

$$\sum_{\substack{n_1, m_1 \\ n_2, m_2}} \Gamma_{n_1 n_2 N}^{m_1 m_2 M} Z_{n_1}^{m_1*}(\mathbf{s}_1) Z_{n_2}^{m_2*}(\mathbf{s}_2) = \frac{\pi}{4} Z_N^{M*} \left( \frac{\mathbf{s}_1 + \mathbf{s}_2}{2} \right) \mathbb{1}_D(\mathbf{s}_1) \mathbb{1}_D(\mathbf{s}_2). \quad (18)$$

(17) and (18) are the counterparts of (12) and (13): the  $\Gamma$ -coefficients play a complementary role. Another important identity is

$$\sum_{nm} Z_n^m(\mathbf{s}) \tilde{Z}_n^{m*}(\mathbf{q}) = \pi \mathbb{1}_D(\mathbf{s}) e^{-2\pi i \mathbf{s} \cdot \mathbf{q}}, \quad (19)$$

from which the following relation follows immediately

$$\sum_{\substack{n_1, m_1 \\ n_2, m_2}} \Gamma_{n_1 n_2 N}^{m_1 m_2 M*} A_{n_1 n_2 N_1}^{m_1 m_2 M_1} = \frac{\pi}{4} \delta_{NN_1} \delta_{MM_1}, \quad (20)$$

and similarly under permutations of  $((n_1, m_1), (n_2, m_2))$ , and  $(N, M)$ .

The derivations of the above identities and contraction identities involving the  $A$ - and  $\Gamma$ -coefficients, as well as their explicit representations, are collected in Appendix A. To the best of our knowledge, several identities derived here do not appear in the existing literature.

We note that identities derived above (e.g. (20)) rely only on completeness and orthogonality of the underlying mode set, and therefore have analogs in other orthonormal bases. The distinctive features of the Zernike representation arise from the specific algebraic structure of the associated coupling coefficients and their radial and azimuthal selection rules.

The  $A$ -coefficients enforce real-space coincidence and Fourier-domain mode addition, while the  $\Gamma$ -coefficients provide the complementary coupling structure connecting real and Fourier representations that will later be shown to govern non-collinear and collinear two-photon correlations, respectively.

## B. Zernike expansion of the pupil function and field representation.

To connect the Zernike-mode formalism with physical optical fields, we represent the generalized pupil function in the Zernike basis. For a circular pupil of radius  $R$ , the complex pupil function can be written as

$$P(R\rho, \theta) = A(R\rho, \theta) \exp[i\Phi(R\rho, \theta)] = \sum_{n=0}^{\infty} \sum_{m=-n}^n b_{nm} Z_n^m(\rho, \theta), \quad (21)$$

where the complex coefficients  $b_{nm}$  account for both phase aberrations and amplitude variations across the pupil. In the special case of a purely phase-aberrated wavefront, this reduces to expansion frequently used in optics

$$\exp[i\Phi(R\rho, \theta)] = \sum_{n=0}^{\infty} \sum_{m=-n}^n a_{nm} Z_n^m(\rho, \theta). \quad (22)$$

with real-valued coefficients  $a_{nm}$  directly associated with specific aberration modes. While the  $a_{nm}$  coefficients admit a direct physical interpretation in terms of classical aberrations, the more general  $b_{nm}$  representation provides a compact and flexible description of realistic optical fields, in which only a limited number of low-order modes typically contribute significantly. A key consequence is that, within the Fraunhofer approximation, a field expanded in Zernike modes in the pupil plane

maps to an image-plane field obtained by replacing each Zernike polynomial by its Fourier–Zernike transform with unchanged expansion coefficients, a property that will be exploited in the following analysis.

### C. Field operators and extended Huygens–Fresnel principle.

We now consider the propagation of optical fields expanded in the Zernike basis through a turbulent medium. Starting from a pupil-plane representation of the field in terms of Zernike modes, we incorporate the effects of atmospheric turbulence using the extended Huygens–Fresnel principle, which provides a statistical description of wave propagation in random media. In this framework, turbulence enters as a stochastic phase perturbation accumulated along the propagation path, allowing ensemble-averaged field correlations to be evaluated analytically. This approach enables a systematic treatment of how Zernike-mode components are modified under propagation while remaining naturally adapted to rotationally symmetric, statistically isotropic turbulence.

Within the extended Huygens–Fresnel formalism, the field propagated from the source plane to a distance  $z$  at transverse coordinate  $\boldsymbol{\rho} = (x, y)$  is expressed as a superposition of secondary wavelets, each acquiring a random, turbulence-induced phase shift

$$U(\boldsymbol{\rho}, z) = \frac{ke^{ikz}}{2\pi iz} \int_D d^2s U_0(\mathbf{s}, 0) e^{i\frac{k|\mathbf{s}-\boldsymbol{\rho}|^2}{2z} + \psi(\boldsymbol{\rho}, \mathbf{s})}, \quad (23)$$

where  $D$  is the pupil domain. In addition to the deterministic Fresnel phase, propagation through the random medium introduces a stochastic contribution  $\psi(\boldsymbol{\rho}, \mathbf{s})$ , which accounts for the cumulative effect of refractive-index fluctuations along the propagation path. This random phase is treated as a statistically homogeneous and isotropic process, so that ensemble-averaged field correlations can be evaluated in terms of the spatial separation of propagation paths rather than individual realizations of the medium.  $\psi(\boldsymbol{\rho}, \mathbf{s}) = \psi_1(\boldsymbol{\rho}, \mathbf{s}) + \psi_2(\boldsymbol{\rho}, \mathbf{s})$  where  $\psi_1(\boldsymbol{\rho}, \mathbf{s})$  and  $\psi_2(\boldsymbol{\rho}, \mathbf{s})$  are first- and second-order perturbations, respectively.

If, in addition to the Fresnel approximation, the stronger Fraunhofer approximation ( $z > ks_{\max}^2/\pi = 4kD/\pi^2$ ) is satisfied, then the field is determined as

$$U(\boldsymbol{\rho}, z) = \frac{ke^{ikz} e^{i\frac{k}{2z}\boldsymbol{\rho}^2}}{2\pi iL} \int_D d^2s U_0(\mathbf{s}, 0) e^{-i\frac{k}{z}\boldsymbol{\rho}\cdot\mathbf{s} + \psi(\boldsymbol{\rho}, \mathbf{s})}. \quad (24)$$

The Fraunhofer representation is particularly simple because a pupil-plane function expressed in Zernike modes  $Z_n^m(\boldsymbol{\rho})$  has an image-plane counterpart obtained simply by substituting their Fourier transforms  $\tilde{Z}_n^m(\mathbf{q})$  for  $Z_n^m(\boldsymbol{\rho})$  [28]. This structure is expected to remain largely intact once weak atmospheric turbulence is incorporated.

With this formalism at hand, we next introduce the turbulence-induced phase distortions into Zernike mode

representation of the field operator [21]. To incorporate this propagation model at the quantum level, we now reformulate the extended Huygens–Fresnel description in terms of field operators. We start with the angular spectrum representation of the field operator at position  $\mathbf{r} = (\boldsymbol{\rho}, z)$  in paraxial approximation

$$\mathbf{E}^{(+)}(\mathbf{r}) = e^{ikz} \int d^2q a(\mathbf{q}) e^{i(\mathbf{q}\cdot\boldsymbol{\rho} - \frac{z}{2k}q^2)} \quad (25)$$

which, in terms of the Zernike mode annihilation operators

$$z_n^m = \frac{1}{\sqrt{\pi}} \int d^2q \tilde{Z}_n^m(\mathbf{q}) a(\mathbf{q}), \quad (26)$$

$|z_n^m\rangle = (z_n^m)^\dagger|0\rangle$ , with  $[a(\mathbf{q}), a^\dagger(\mathbf{q}')] = \delta(\mathbf{q} - \mathbf{q}')$  and  $[\tilde{z}_n^m, \tilde{z}_{n'}^{m'}] = \delta_{mm'}\delta_{nn'}$ , has the form [21]

$$\mathbf{E}^{(+)}(\mathbf{r}) = \frac{ke^{ikz}}{2iz\pi^{\frac{3}{2}}} \sum_{mn} \tilde{z}_n^m \int d^2s Z_n^m(\mathbf{s}) e^{i\frac{ik}{2z}|\boldsymbol{\rho}-\mathbf{s}|^2}. \quad (27)$$

In the quantum description, the classical Zernike expansion coefficients  $b_{nm}$  in (21) are promoted to annihilation operators  $\tilde{z}_n^m$ , preserving the Zernike-mode structure of the field while enabling a direct operator-based treatment of propagation and detection.

In the Fraunhofer zone the field operator assumes the form,

$$\mathbf{E}^{(+)}(\mathbf{r}) = \frac{ke^{ikz + i\frac{k\rho^2}{2z}}}{iz\sqrt{\pi}} \sum_{mn} \tilde{Z}_n^m(\boldsymbol{\rho}) \tilde{z}_n^m, \quad (28)$$

where  $\boldsymbol{\rho} = 2\pi\mathbf{q}z/k$  is the position at the detection plane corresponding to the Fourier component  $\mathbf{q}$ . For single-photon or collinear two-photon detection scenarios, factors  $e^{ikz}$  and  $e^{i\frac{k\rho^2}{2z}}$  are irrelevant. Only for the joint two-photon detection case, they must either be retained or assumed to be removed by adaptive optics. To account for the effect of the medium on the Fraunhofer pattern, one can add the complex random phase  $\psi$  to the propagator in (4)

$$\mathbf{E}^{(+)}(\mathbf{r}) = \frac{ke^{ikz}}{2iz\pi^{\frac{3}{2}}} \sum_{mn} \tilde{z}_n^m \int d^2s Z_n^m(\mathbf{s}) e^{i\frac{k}{2z}\mathbf{s}\cdot\boldsymbol{\rho} + \psi(\boldsymbol{\rho}, \mathbf{s})}. \quad (29)$$

### III. PROPAGATION AND DETECTION OF TWO-PHOTON ZERNIKE STATES

We now apply the propagation formalism developed in Sec. II to spatially entangled degenerate ( $\omega_1 = \omega_2$ ) photon pairs generated via spontaneous parametric down-conversion in the paraxial, monochromatic approximations [29]:

$$|\psi\rangle = \iint d^2q_1 d^2q_2 \tilde{E}_p(\mathbf{q}_1 + \mathbf{q}_2) \times \text{sinc}\left(\frac{L(|\mathbf{q}_1 - \mathbf{q}_2|^2)}{4K}\right) \hat{a}^\dagger(\mathbf{q}_1) \hat{a}^\dagger(\mathbf{q}_2) |0\rangle, \quad (30)$$

where  $\mathbf{q}_1$  and  $\mathbf{q}_2$  are the transverse components of the down-converted wave vectors,  $\tilde{E}_p(\mathbf{q})$  is the angular spectrum of the pump-beam,  $k_p$  is the wave number of the pump-beam,  $L$  the crystal thickness. The state (30) written in the Zernike mode basis has the form [21]

$$|\psi\rangle = \sum_{\substack{m_1 m_2 \\ n_1 n_2}} \zeta_{n_1 n_2}^{m_1 m_2} |z_{n_1}^{m_1}, z_{n_2}^{m_2}\rangle, \quad (31)$$

where  $\zeta_{n_1 n_2}^{m_1 m_2} = \langle z_{n_1}^{m_1}, z_{n_2}^{m_2} | \psi \rangle$ . The two-photon state in (31) provides the setting in which the  $A$ - and  $\Gamma$ -structures discussed in Sec. II naturally enter the two-photon problem. In particular, interesting subclasses arise when the coefficients  $\zeta_{n_1 n_2}^{m_1 m_2}$  acquire the structured forms associated with the  $A$ - and  $\Gamma$ -coefficients, leading to the following two-photon states:

$$\begin{aligned} |\psi\rangle_A &= \sum_{\substack{m_1 m_2 \\ n_1 n_2}} A_{n_1 n_2 N}^{m_1 m_2 M} |z_{n_1}^{m_1}, z_{n_2}^{m_2}\rangle \\ &= \frac{1}{\pi} \sum_{\substack{m_1 m_2 \\ n_1 n_2}} A_{n_1 n_2 N}^{m_1 m_2 M} \iint d^2 q_1 d^2 q_2 \\ &\quad \times \tilde{Z}_{n_1}^{m_1}(\mathbf{q}_1) \tilde{Z}_{n_2}^{m_2}(\mathbf{q}_2) a^\dagger(\mathbf{q}_1) a^\dagger(\mathbf{q}_2) |0\rangle \\ &= \iint d^2 q_1 d^2 q_2 \tilde{Z}_N^M(\mathbf{q}_1 + \mathbf{q}_2) a^\dagger(\mathbf{q}_1) a^\dagger(\mathbf{q}_2) |0\rangle, \end{aligned} \quad (32)$$

which corresponds to the thin-crystal approximation of SPDC, with  $\tilde{E}_p(\mathbf{q}_1 + \mathbf{q}_2) = \tilde{Z}_N^M(\mathbf{q}_1 + \mathbf{q}_2)$ , and

$$\begin{aligned} |\psi\rangle_\Gamma &= \sum_{\substack{m_1 m_2 \\ n_1 n_2}} \Gamma_{n_1 n_2 N}^{m_1 m_2 M} |z_{n_1}^{m_1}, z_{n_2}^{m_2}\rangle \\ &= \frac{1}{\pi} \sum_{\substack{m_1 m_2 \\ n_1 n_2}} \Gamma_{n_1 n_2 N}^{m_1 m_2 M} \iint d^2 q_1 d^2 q_2 \\ &\quad \times \tilde{Z}_{n_1}^{m_1}(\mathbf{q}_1) \tilde{Z}_{n_2}^{m_2}(\mathbf{q}_2) a^\dagger(\mathbf{q}_1) a^\dagger(\mathbf{q}_2) |0\rangle \\ &= \int d^2 q \tilde{Z}_N^M(2\mathbf{q}) \left( \int d^2 q_1 \tilde{Z}_0^0(\mathbf{q} - \mathbf{q}_1) a^\dagger(\mathbf{q}_1) \right) \\ &\quad \times \left( \int d^2 q_2 \tilde{Z}_0^0(\mathbf{q} - \mathbf{q}_2) a^\dagger(\mathbf{q}_2) \right) |0\rangle \\ &\equiv \int d^2 q \tilde{Z}_N^M(2\mathbf{q}) \left( \hat{\zeta}^\dagger(\mathbf{q}) \right)^2 |0\rangle, \end{aligned} \quad (34)$$

where (13) and (17) were used. This state is a superposition of two-photon states where both photons have passed through an aperture  $Z_0^0$ , with pump envelope  $\tilde{Z}_N^M(2\mathbf{q})$ . Note that, for a pump with  $N = M = 0$ , the state (34) is separable in the Zernike-mode basis. This does not contradict the non-separable structure of the transverse-momentum representation (35), since the mapping between the two is not a local single-photon basis change: the kernel  $\Gamma$  couples the two photons collectively, leading to the perfectly correlated form in Eq. (35).

For collinear joint two-photon detection, a Zernike-mode measurement basis onto which the propagated

SPDC state will be projected is

$$\begin{aligned} |\phi\rangle &= \int d^2 q \tilde{Z}_{n_1}^{m_1}(\mathbf{q}) \tilde{Z}_{n_2}^{m_2}(\mathbf{q}) a^\dagger(\mathbf{q}) a^\dagger(\mathbf{q}) |0\rangle \\ &= \frac{4}{\pi} \sum_{\substack{nn'n'' \\ mm'm''}} \Gamma_{n_1 n_2 N}^{m_1 m_2 m} |z_{n'}^{m'}, z_{n''}^{m''}\rangle \\ &\quad \times \int d^2 q \tilde{Z}_n^m(2\mathbf{q}) \tilde{Z}_{n'}^{m'*}(\mathbf{q}) \tilde{Z}_{n''}^{m''*}(\mathbf{q}) \\ &= 4 \sum_{\substack{nn'n'' \\ mm'm''}} \Gamma_{n_1 n_2 N}^{m_1 m_2 m} \Gamma_{n' n'' N}^{m' m'' m*} |z_{n'}^{m'}, z_{n''}^{m''}\rangle, \end{aligned} \quad (36)$$

where we used Eqs. (14), (26) and (16). Note that the expansion coefficients of (34) are given by  ${}_A\langle\psi|\phi\rangle$ :

$$\begin{aligned} {}_A\langle\psi|\phi\rangle &= 8 \sum_{\substack{nn'n'' \\ mm'm''}} \Gamma_{n_1 n_2 N}^{m_1 m_2 m} \Gamma_{n' n'' N}^{m' m'' m*} A_{n' n'' N}^{m' m'' M} \\ &= 8 \Gamma_{n_1 n_2 N}^{m_1 m_2 M}, \end{aligned} \quad (37)$$

following from the use of the identity in (20), which now provides the link between non-collinear and collinear Zernike-mode structures.

To connect the propagated two-photon state with measurable quantities, we construct the two-photon detection amplitude

$$\mathcal{A}(\boldsymbol{\rho}_1, \boldsymbol{\rho}_2) = \langle 0 | \hat{E}^{(+)}(\boldsymbol{\rho}_2) \hat{E}^{(+)}(\boldsymbol{\rho}_1) | \psi \rangle \quad (38)$$

with the help of Eqs. (29) and (31):

$$\mathcal{A}(\boldsymbol{\rho}_1, \boldsymbol{\rho}_2) \propto \sum_{\substack{m_1 n_1 \\ m_2 n_2}} \zeta_{n_1 n_2}^{m_1 m_2} \mathcal{J}_{m_1 n_1}(\boldsymbol{\rho}_1) \mathcal{J}_{m_2 n_2}(\boldsymbol{\rho}_2), \quad (39)$$

with the proportionality constant  $-k^2 e^{2ikz} / (2z^2 \pi^3)$  and mode-filtered turbulent propagators

$$\mathcal{J}_{mn}(\mathbf{r}) \equiv \int d^2 s Z_n^m(\mathbf{s}) e^{i \frac{k}{z} \mathbf{s} \cdot \boldsymbol{\rho} + \psi(\mathbf{s}, \boldsymbol{\rho})}. \quad (40)$$

(39) is the far-field representation of the two-photon detection amplitude. In the thin-crystal approximation SPDC, for a pump profile prepared in a single Zernike mode  $Z_N^M$ , the detection amplitude simplifies considerably:

$$\begin{aligned} \mathcal{A}_N^M(\boldsymbol{\rho}_1, \boldsymbol{\rho}_2) &\propto \sum_{\substack{m_1 n_1 \\ m_2 n_2}} A_{n_1 n_2 N}^{m_1 m_2 M} \mathcal{J}_{m_1 n_1}(\boldsymbol{\rho}_1) \mathcal{J}_{m_2 n_2}(\boldsymbol{\rho}_2) \\ &= \int d^2 s Z_N^M(\mathbf{s}) e^{i \frac{k}{z} \mathbf{s} \cdot (\boldsymbol{\rho}_1 + \boldsymbol{\rho}_2) + \psi(\mathbf{s}, \boldsymbol{\rho}_1) + \psi(\mathbf{s}, \boldsymbol{\rho}_2)}, \end{aligned} \quad (41)$$

where we used (12).

### A. No-turbulence limit and recovery of exact selection rules.

Before analyzing the effects of atmospheric turbulence, it is instructive to consider the no-turbulence

limit, in which the stochastic phase perturbation vanishes,  $\psi(\mathbf{s}, \boldsymbol{\rho}) = 0$ . In this case, free-space propagation reduces to deterministic Fraunhofer diffraction, and the propagated field operators preserve the Zernike-mode operator expansion introduced in Sec. II.

$$\begin{aligned} \mathcal{A}_N^M(\boldsymbol{\rho}_1, \boldsymbol{\rho}_2) &\propto \sum_{\substack{m_1 n_1 \\ m_2 n_2}}^{m_1 m_2 M} A_{n_1 n_2 N}^{m_1 m_2 M} \tilde{Z}_{n_1}^{m_1}(\boldsymbol{\rho}_1) \tilde{Z}_{n_2}^{m_2}(\boldsymbol{\rho}_2) \\ &= \tilde{Z}_N^M(\boldsymbol{\rho}_1 + \boldsymbol{\rho}_2), \end{aligned} \quad (42)$$

where the identity (13) has been applied in the second equality. Eq. (42) show that in the absence of turbulence the two-photon detection amplitude reduces to a correlation beam [29] governed by the  $A$ -coefficients.

The joint probability for a pair of photons in modes  $z_{N_1}^{M_1}$  and  $z_{N_2}^{M_2}$  can be calculated as follows [30]

$$\begin{aligned} P_N^M(z_{N_1}^{M_1}, z_{N_2}^{M_2}) &\propto \\ &\left\langle \left| \iint d^2 \rho_1 d^2 \rho_2 \tilde{Z}_{N_1}^{M_1*}(\boldsymbol{\rho}_1) \tilde{Z}_{N_2}^{M_2*}(\boldsymbol{\rho}_2) \mathcal{A}_N^M(\boldsymbol{\rho}_1, \boldsymbol{\rho}_2) \right|^2 \right\rangle. \end{aligned} \quad (43)$$

The normalization factor is

$$\mathcal{N} = \frac{1}{\sqrt{|\langle z_{n_1}^{m_1} | \psi \rangle|^2 |\langle z_{n_2}^{m_2} | \psi \rangle|^2}}. \quad (44)$$

Without turbulence, (43) reduces, as it should, to (see appendix B)

$$P_{NM}^{\text{no turb}}(z_{N_1}^{M_1}, z_{N_2}^{M_2}) = \begin{cases} |A_{N_1 N_2 N}^{M_1 M_2 M}|^2, & \boldsymbol{\rho}_1 \neq \boldsymbol{\rho}_2, \\ |\Gamma_{N_1 N_2 N}^{M_1 M_2 M}|^2, & \boldsymbol{\rho}_1 = \boldsymbol{\rho}_2. \end{cases} \quad (45)$$

Recall from the representations given in Appendix A 1,

$$\begin{aligned} A_{N_1 N_2 N}^{M_1 M_2 M} &= 0 \quad \text{for } N > N_1 + N_2, \text{ whereas} \\ \Gamma_{N_1 N_2 N}^{M_1 M_2 M} &= 0 \quad \text{for } N < N_1 + N_2. \end{aligned}$$

Accordingly, in the far-field, for a pump prepared in a single Zernike mode  $Z_N^M$ , the mode-coupling structure enforces exact selection rules: conservation of azimuthal order  $M_1 + M_2 = M$ , together with the radial constraint  $N \leq N_1 + N_2$  for the  $A$ -coefficients, and  $N \geq N_1 + N_2$  for the  $\Gamma$  (subject to the usual parity condition).

### B. Ensemble-averaged two-photon detection probability in turbulence.

We now incorporate the effects of atmospheric turbulence by performing an ensemble average over the random phase perturbation  $\psi(\boldsymbol{\rho}, \mathbf{s})$ . The following analysis assumes weak-to-moderate turbulence, such that the

extended Huygens–Fresnel approximation remains valid and ensemble averages are dominated by second-order phase statistics; technical details are given in Appendix C. In contrast to the no-turbulence case, the joint two-photon detection probability is no longer determined solely by deterministic Fraunhofer propagation, but depends on statistical correlations of the turbulent medium. The probability  $P_N^M(z_{N_1}^{M_1}, z_{N_2}^{M_2})$  for the case of collinear two photon amplitude  $\mathcal{A}$  in thin crystal approximation is calculated in Appendix C:

$$P_N^M(z_{N_1}^{M_1}, z_{N_2}^{M_2}) = \sum_{n_1 n_2} F_{n_1} F_{n_2}^* \sum_{n_5} G_{n_5}^0 A_{n_1 n_2 n_5}^{m_1, -m_1, 0}, \quad (46)$$

where

$$F_n = \sum_{n'} \Gamma_{N_1 N_2 n'}^{M_1 M_2, M_1 + M_2} \Gamma_{n' N n}^{-M_1 - M_2, M, M - M_1 - M_2}, \quad (47)$$

and

$$\begin{aligned} G_{n_5}^{m_5}(\gamma) &= \int d^2 u e^{-2\frac{\gamma k}{z} u^2} \tilde{Z}_{n_5}^{m_5} \left( \frac{4kR}{z} \mathbf{u} \right) \\ &= 2\pi \delta_{m_5 0} i^{n_5} \sqrt{n_5 + 1} \frac{\pi z}{4\gamma k} \left( \sqrt{\frac{8\pi^2 k R^2}{\gamma z}} \right)^{n_5} \\ &\times \frac{\Gamma\left(\frac{n_5 + 2}{2}\right)}{\Gamma(n_5 + 2)} {}_1F_1\left(\frac{n_5 + 2}{2}; n_5 + 2; -\frac{8\pi^2 k R^2}{\gamma z}\right), \end{aligned} \quad (48)$$

and  ${}_1F_1$  is the confluent hypergeometric function, with  $\gamma \equiv 0.4 (\sigma_R^2)^{6/5}$ ,  $\sigma_R^2$  being the Rytov variance, a measure of the turbulence strength.

## IV. DISCUSSION

A central result of this work is the exact analytical reduction of the continuous extended Huygens–Fresnel propagation integrals into a discrete, finite-dimensional algebraic framework. This formulation provides deep physical insight into a closed-form discrete algebraic framework.

In the ideal vacuum limit ( $\sigma_R \rightarrow 0$ ), the turbulence tensor  $G_{n_5}^0(\gamma)$  reduces analytically to the origin-evaluation of the spatial Zernike polynomials. Within our algebraic framework, this rigorously collapses the probability down to a single  $|\Gamma_{N_1 N_2 N}^{M_1 M_2 M}|^2$ . As shown in the  $\sigma_R = 0.0$  panel of Fig. 1, this perfectly recovers the exact momentum-matching constraints of free-space diffraction: strict azimuthal conservation ( $M = M_1 + M_2$ ) and the radial triangle inequality ( $N \geq N_1 + N_2$ ). The absence of numerical artifacts in this limit highlights the exactness of the discrete tensor collapse.

When atmospheric turbulence is introduced ( $\sigma_R > 0$ ), the discrete structure clearly delineates the breakdown of global selection rules. Because a single realization of a turbulent phase screen physically breaks the azimuthal

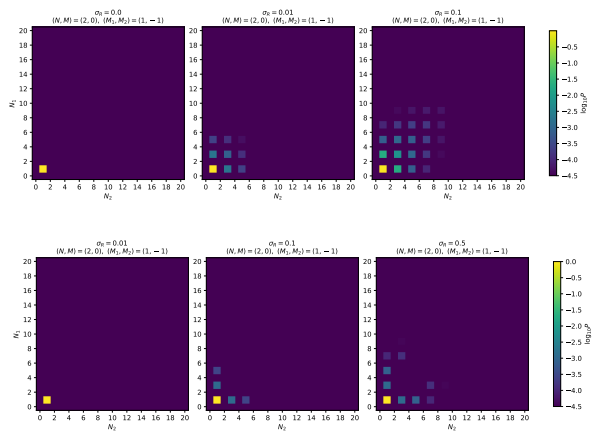


FIG. 1: *Top Row*: Radial-mode correlations in Zernike-entangled photon pairs under varying turbulence strengths. Shown is the base-10 logarithm of the normalized joint detection probability  $P_N^M(\tilde{Z}_{N_1}^{M_1}, \tilde{Z}_{N_2}^{M_2})$ . The color scale is lower-bounded at  $10^{-4.5}$  to isolate physically meaningful crosstalk from negligible numerical background. Rows correspond to fixed detector azimuthal indices  $(M_1, M_2) = (1, -1)$ . Columns compare increasing turbulence strengths for a pump mode  $(N, M) = (2, 0)$ . Left ( $\sigma_R = 0.0$ ): In a perfect vacuum, exact momentum-matching and Zernike selection rules perfectly restrict the transition to a single state ( $N_1 = 1, N_2 = 1$ ). Center and Right ( $\sigma_R = 0.01$  and  $0.1$ ): Increasing turbulence relaxes the radial-order constraints and breaks the macroscopic azimuthal selection rule, forming an extended, exponentially decaying distribution across higher radial orders, reflecting the relaxation of the strict free-space Zernike constraints. *Bottom Row*: Ideal partial AO is mathematically modeled by truncating the lowest-order macroscopic modes from the turbulence tensor ( $n_5 > 6$  in (46), correcting up to primary spherical aberration). This truncation perfectly restores the free-space limit at  $\sigma_R = 0.01$  and heavily suppresses crosstalk at weak-to-moderate turbulence ( $\sigma_R = 0.1$ ). Even under moderate-to-strong turbulence ( $\sigma_R = 0.5$ ), the target correlation peak remains highly dominant. The residual leakage is confined to adjacent modes, demonstrating that high-frequency turbulent eddies cannot efficiently drive simultaneous, multi-mode radial scattering. *Parameters*:  $k = 10^7 \text{ m}^{-1}$ ,  $z = 5 \times 10^3 \text{ m}$ ,  $R = 5 \times 10^{-3} \text{ m}$ .

symmetry of the propagating wavefront, the macroscopic azimuthal selection rule is violated ( $M \neq M_1 + M_2$ ). This breakdown represents the onset of orbital angular momentum (OAM) crosstalk, a well-documented source of decoherence in turbulent free-space channels [17, 18]. However, while prior studies utilizing LG modes observe this OAM crosstalk as a broad, diffusive spread across azimuthal indices [18], our formalism reveals that in the Zernike basis, this scattering remains hierarchically structured. The azimuthal leakage is explicitly routed

by the  $\Gamma$  tensors and geometrically bounded by the spatial overlap  $A$ -tensors. This sequence of tensor contractions explicitly governs the breakdown of macroscopic OAM conservation, quantifying the resulting turbulence-induced azimuthal crosstalk.

As visualized in Fig. 1 (Top Row), the probability is redistributed along increasing total radial orders, showing an outward diagonal decay along  $N_1 + N_2$ . Unlike the diffusive, unbounded mode-mixing observed in Hermite- or Laguerre-Gaussian bases, the Zernike mode coupling is hierarchically constrained. Because atmospheric turbulence is natively well-described by low-order aberrations (piston, tilt, astigmatism), its dominant effects map highly efficiently onto the lowest-order  $G$ -tensor components. This structured coupling implies that partial adaptive optics—targeting only the first few Zernike modes—can recover a disproportionately large fraction of the initial quantum spatial correlations.

Finally, a distinct advantage of our discrete algebraic framework is its native capacity to model partial adaptive optics (AO) without requiring computationally expensive phase-screen subtractions. In our formalism, the turbulence tensor  $G_{n_5}^0(\gamma)$  acts as a discrete modal filter, dictating the statistical weight of the  $n_5$ -th aberration in driving intermodal crosstalk. To mathematically model an ideal AO system that perfectly compensates for low-order wavefront distortions up to a radial order  $N_{AO}$ , we simply apply a high-pass truncation to the transition probability network, restricting the sum in Eq. (46) to  $n_5 > N_{AO}$ . Fig. 1 (Bottom Row) illustrates the physical consequence of this truncation. It shows the unaberrated baseline alongside the characteristic diagonal crosstalk induced by uncorrected turbulence. We apply a simulated AO correction up to primary spherical aberration ( $N_{AO} = 6$ ). By merely filtering out these macroscopic, low-order modes, the extended diagonal crosstalk is almost entirely eliminated. Even when subjected to stronger turbulence ( $\sigma_R = 0.5$ ), the correlation peak at ( $N_1 = 1, N_2 = 1$ ) remains intact. Notably, the residual high-frequency turbulence only drives faint scatterings into adjacent modes, proving that the bulk of two-photon decoherence in the Zernike basis is strictly driven by the lowest spatial frequencies of the Kolmogorov spectrum.

## V. CONCLUSION

We have developed an exact, discrete algebraic framework for the propagation and detection of Zernike-entangled two-photon states through atmospheric turbulence. By analytically resolving the extended Huygens-Fresnel integrals into a discrete sequence of spatial ( $A$ ) and Fourier-domain ( $\Gamma$ ) overlaps, and turbulent ( $G$ ) tensors, we bypassed the severe numerical limitations of highly oscillatory continuous path integrals. Our results demonstrate that turbulence-induced decoherence in the Zernike basis is highly structured. We explicitly showed how the macroscopic breakdown of OAM conservation

mathematically coexists with the statistical isotropy of the turbulent medium. Furthermore, we showed that the degradation hierarchy is heavily dominated by low-order modes, reflecting the aberration-like nature of atmospheric phase distortions. These findings establish the Zernike basis not merely as a mathematical alternative to LG/HG modes, but as a naturally optimal representation for characterizing and mitigating decoherence in free-space quantum communication channels. Future work will extend this algebraic framework to strong-turbulence regimes and broadband sources. Furthermore, we demonstrated that this discrete tensor formalism provides a closed algebraic method for modeling par-

tial adaptive optics. By applying a simple high-pass truncation to the discrete turbulence tensor ( $G_{n_5}^0$ ), we showed that correcting aberrations up to order  $N_{AO} = 6$  is sufficient to almost entirely suppress widespread radial crosstalk, even in stronger turbulence regimes ( $\sigma_R = 0.5$ ). This confirms that quantum decoherence in the Zernike basis is heavily dominated by macroscopic, low-order phase distortions, offering a highly efficient theoretical blueprint for optimizing free-space quantum channels.

**Acknowledgment.** We thank Varazdat Stepanyan for discussions. This work was supported by HESC (Higher Education and Science Committee) of Armenia, Grants No. 24FP-1F030 and 23/2IRF-1C003.

- 
- [1] L. Allen, M. W. Beijersbergen, R. J. C. Spreeuw, and J. P. Woerdman, Orbital angular momentum of light and the transformation of Laguerre-Gaussian laser modes, *Phys. Rev. A* **45**, 8185 (1992).
- [2] V. Y. Bazhenov, M. S. Soskin, and M. V. Vasnetsov, Screw dislocations in light wavefronts, *J. Mod. Opt.* **39**, 985 (1992).
- [3] M. W. Beijersbergen, L. Allen, H. E. L. O. van der Veen, and J. P. Woerdman, Astigmatic laser mode converters and transfer of orbital angular momentum, *Opt. Commun.* **96**, 123 (1993).
- [4] M. J. Padgett and J. Courtial, Poincaré sphere equivalent for light beams containing orbital angular momentum, *Opt. Lett.* **24**, 430 (1999).
- [5] G. S. Agarwal,  $Su(2)$  structure of the poincaré sphere for light beams with orbital angular momentum, *Opt. Soc. Am. A* **16**, 2914 (1999).
- [6] A. Mair, A. Vaziri, G. Weihs, and A. Zeilinger, Entanglement of the orbital angular momentum states of photons, *Nature (London)* **412**, 313 (2001).
- [7] A. Vaziri, G. Weihs, and A. Zeilinger, Experimental two-photon, three-dimensional entanglement for quantum communication, *Phys. Rev. Lett.* **89**, 240401 (2002).
- [8] S. Goel, B. Ghosh, and M. Malik, Quantum information processing with spatially structured light, *Advanced Photonics* **8**, 014005 (2025).
- [9] S. P. Walborn, A. N. de Oliveira, R. S. Thebaldi, and C. H. Monken, Entanglement and conservation of orbital angular momentum in spontaneous parametric down-conversion, *Phys. Rev. A* **69**, 023811 (2004).
- [10] S. P. Walborn, S. Pádua, and C. H. Monken, Conservation and entanglement of Hermite-Gaussian modes in parametric down-conversion, *Phys. Rev. A* **71**, 053812 (2005).
- [11] L. C. Andrews and R. L. Phillips, *Laser Beam Propagation Through Random Media* (SPIE, 2005).
- [12] R. W. Boyd, B. Rodenburg, M. Mirhosseini, and S. M. Barnett, Influence of atmospheric turbulence on the propagation of quantum states of light using plane-wave encoding, *Opt. Express* **19**, 18310 (2011).
- [13] Y. Ren, H. Huang, G. Xie, N. Ahmed, Y. Yan, B. I. Erkmen, N. Chandrasekaran, M. P. J. Lavery, N. K. Steinhoff, M. Tur, S. Dolinar, M. Neifeld, M. J. Padgett, R. W. Boyd, J. H. Shapiro, and A. E. Willner, Atmospheric turbulence effects on the performance of a free space optical link employing orbital angular momentum multiplexing, *Opt. Lett.* **38**, 4062 (2013).
- [14] M. Krenn, R. Fickler, M. Fink, J. Handsteiner, M. Malik, T. Scheidl, R. Ursin, and A. Zeilinger, Communication with spatially modulated light through turbulent air across vienna, *New Journal of Physics* **16**, 113028 (2014).
- [15] D. Vasylyev, A. A. Semenov, and W. Vogel, Atmospheric quantum channels with weak and strong turbulence, *Physical Review Letters* **117**, 090501 (2016).
- [16] M. Ghalaii and S. Pirandola, Quantum communications in a moderate-to-strong turbulent atmosphere, *Commun. Physics* **5**, 38 (2022).
- [17] C. Paterson, Atmospheric turbulence and orbital angular momentum of single photons for optical communication, *Phys. Rev. Lett.* **94**, 153901 (2005).
- [18] G. A. Tyler and R. W. Boyd, Influence of atmospheric turbulence on the propagation of quantum states of light carrying orbital angular momentum, *Opt. Lett.* **34**, 142 (2009).
- [19] H. Avetisyan and C. H. Monken, Higher order correlation beams in atmosphere under strong turbulence conditions, *Opt. Express* **24**, 2318 (2016).
- [20] H. Avetisyan and C. H. Monken, Mode analysis of higher-order transverse-mode correlation beams in a turbulent atmosphere, *Opt. Lett.* **42**, 101 (2017).
- [21] H. Avetisyan and G. Nikoghosyan, Quantum aberrations: Entangling photons with Zernike polynomials, *Phys. Rev. A* **112**, 043714 (2025).
- [22] R. J. Noll, Zernike polynomials and atmospheric turbulence, *J. Opt. Soc. Am.* **66**, 207 (1976).
- [23] S. N. Bezdidko, The use of Zernike polynomials in optics, *Sov. J. Opt. Technol.* **41**, 425 (1974).
- [24] D. L. Fried, Statistics of a geometric representation of wavefront distortion, *J. Opt. Soc. Am.* **55**, 1427 (1965).
- [25] W. J. Tango, The circle polynomials of Zernike and their application in optics, *Applied Physics* **13**, 327 (1977).
- [26] E. C. Kintner and R. M. Sillitto, A new “analytic” method for computing the optical transfer function, *Opt. Acta* **23**, 607 (1976).
- [27] A. J. E. M. Janssen, New analytic results for the Zernike circle polynomials from a basic result in the Nijboer-Zernike diffraction theory, *J. Eur. Opt. Soc.-Rapid Publ.* **6**, 11028 (2011).
- [28] E. C. Kintner, Some comments on the use of the Zernike polynomials in optics, *Opt. Commun.* **18**, 235 (1976).

- [29] S. Walborn, C. Monken, S. Pádua, and P. Souto Ribeiro, Spatial correlations in parametric down-conversion, *Phys. Rep.* **495**, 87 (2010).
- [30] S. Franke-Arnold, S. M. Barnett, M. J. Padgett, and L. Allen, Two-photon entanglement of orbital angular momentum states, *Phys. Rev. A.* **65**, 033823 (2002).
- [31] D. A. Varshalovich, A. N. Moskalev, and V. K. Khersonskii, *Quantum theory of angular momentum* (World Scientific, 1988).
- [32] I. S. Gradshteyn and I. M. Ryzhik, *Table of Integrals, Series, and Products*, 8th ed. (Elsevier, USA, 2015).

## Appendix A: Derivation and summary of Zernike and Fourier–Zernike identities

### 1. Representations of $A$ and $\Gamma$

For practical evaluation, both  $A$ – and  $\Gamma$ –sets admit compact representations in terms of Clebsch–Gordan coefficients ( $A$ ) and triple-Bessel integrals ( $\Gamma$ ), which we summarize next.

*Representation for  $A$ .* The coefficients  $A$  are given by the Clebsch–Gordan coefficients [25, 31]

$$A_{n_1 n_2 n_3}^{m_1 m_2 m_3} = \sqrt{\frac{(n_1 + 1)(n_2 + 1)}{n_3 + 1}} \left| C_{\frac{n_1}{2} \frac{m_1}{2} \frac{n_2}{2} \frac{m_2}{2}}^{\frac{n_3}{2} \frac{m_3}{2}} \right|^2, \quad (\text{A1})$$

which are non-vanishing only when  $n_1, n_2, n_3$  are non-negative integers or half-integers, such that  $n_1 + n_2 + n_3$  is even while satisfying the triangle conditions  $|n_r - n_s| \leq n_t \leq n_r + n_s$  for any permutation  $r, s, t$  of 1, 2, 3, and when  $m_r = -n_r, -n_r + 1, \dots, n_r - 1, n_r$ ,  $r = 1, 2, 3$ , with  $m_1 + m_2 - m_3 = 0$ .

*Representation for  $\Gamma$ .* The  $\Gamma$ –coefficients are evaluated as [27]:

$$\begin{aligned} \Gamma_{N_1 N_2 n}^{m m' m''} &= \frac{\delta_{m'', m+m'}}{\pi} i^{N_1 + N_2 - n} \sqrt{\frac{n + 1}{(N_1 + 1)(N_2 + 1)}} \\ &\times \left[ Q_{N_1 N_2}^{n+1}(1, 1, 2) + Q_{N_1+2, N_2}^{n+1}(1, 1, 2) + Q_{N_1, N_2+2}^{n+1}(1, 1, 2) + Q_{N_1+2, N_2+2}^{n+1}(1, 1, 2) \right], \end{aligned} \quad (\text{A2})$$

with  $N_1 + N_2 - n$  even, which implies that  $\Gamma$ s are also real, and  $Q_{ij}^k(a, b, c) = \int_0^\infty du J_i(au) J_j(bu) J_k(cu)$ , so that

$$Q_{N_1 N_2}^{n+1}(1, 1, 2) = \begin{cases} \frac{\left(\frac{1}{2}(n+N_1+N_2)\right)! \left(\frac{1}{2}(n-N_1-N_2)\right)!}{\left(\frac{1}{2}(n-N_1+N_2)\right)! \left(\frac{1}{2}(n+N_1-N_2)\right)!} \frac{1}{2^{2N_1+2N_2+1}} P_{\frac{n-N_1-N_2}{2}}^{(N_1, N_2)}(0) P_{\frac{n-N_1-N_2}{2}}^{(N_2, N_1)}(0), & n \geq N_1 + N_2, \\ 0, & n < N_1 + N_2, \end{cases} \quad (\text{A3})$$

$P_k^{(\alpha, \beta)}$  being the Jacobi polynomial.

### 2. New identities

Using the completeness of the Zernike polynomials and the definition (10) of the  $A$ –coefficients, the following summed product collapses to a  $Z_N^M$  projector:

$$\begin{aligned} \sum_{\substack{n_1, m_1 \\ n_2, m_2}} A_{n_1 n_2 N}^{m_1 m_2 M} Z_{n_1}^{m_1}(\mathbf{s}_1) Z_{n_2}^{m_2}(\mathbf{s}_2) &= \frac{1}{\pi} \int d^2 s Z_N^M(\mathbf{s}) \left[ \sum_{n_1, m_1} Z_{n_1}^{m_1}(\mathbf{s}_1) Z_{n_1}^{m_1}(\mathbf{s})^* \right] \left[ \sum_{n_2, m_2} Z_{n_2}^{m_2}(\mathbf{s}_2) Z_{n_2}^{m_2}(\mathbf{s})^* \right] \\ &= \int d^2 s Z_N^M(\mathbf{s}) \left[ \sum_{n_1, m_1} Z_{n_1}^{m_1}(\mathbf{s}_1) Z_{n_1}^{m_1}(\mathbf{s})^* \right] \delta_D(\mathbf{s}_2 - \mathbf{s}) = \pi Z_N^M(\mathbf{s}_2) \left[ \sum_{n_1, m_1} Z_{n_1}^{m_1}(\mathbf{s}_1) Z_{n_1}^{m_1}(\mathbf{s}_2)^* \right] = \pi Z_N^M(\mathbf{s}_1) \delta_D(\mathbf{s}_1 - \mathbf{s}_2). \end{aligned} \quad (\text{A4})$$

The identity should be understood in the distributional sense under integration against admissible disk-supported test functions. In the Fourier domain, we have

$$\sum_{\substack{n_1, m_1 \\ n_2, m_2}} A_{n_1 n_2 N}^{m_1 m_2 M} \tilde{Z}_{n_1}^{m_1}(\boldsymbol{\rho}_1) \tilde{Z}_{n_2}^{m_2}(\boldsymbol{\rho}_2) = \pi \tilde{Z}_N^M(\boldsymbol{\rho}_1 + \boldsymbol{\rho}_2). \quad (\text{A5})$$

Similarly, using the definition (16) of  $\Gamma$  we have

$$\begin{aligned} \sum_{\substack{n_1, m_1 \\ n_2, m_2}} \Gamma_{n_1 n_2 N}^{m_1 m_2 M} \tilde{Z}_{n_1}^{m_1*}(\mathbf{q}_1) \tilde{Z}_{n_2}^{m_2*}(\mathbf{q}_2) &= \frac{1}{\pi} \int d^2 q \tilde{Z}_N^{M*}(2\mathbf{q}) \left[ \sum_{n_1 m_1} \tilde{Z}_{n_1}^{m_1}(\mathbf{q}) \tilde{Z}_{n_1}^{m_1*}(\mathbf{q}_1) \right] \left[ \sum_{n_2 m_2} \tilde{Z}_{n_2}^{m_2}(\mathbf{q}) \tilde{Z}_{n_2}^{m_2*}(\mathbf{q}_2) \right] \\ &= \pi \int d^2 q \tilde{Z}_N^{M*}(2\mathbf{q}) \tilde{Z}_0^0(\mathbf{q} - \mathbf{q}_1) \tilde{Z}_0^0(\mathbf{q} - \mathbf{q}_2). \end{aligned} \quad (\text{A6})$$

As the Fourier transform of the product  $\tilde{Z}_N^{M*}(2\mathbf{q}) \tilde{Z}_0^0(\mathbf{q} - \mathbf{q}_1)$  is not supported on the unit disk, the projector  $\tilde{Z}_0^0(\mathbf{q} - \mathbf{q}_2)$  does not act as a delta function. Now, double Fourier transforming (A6), we get

$$\sum_{\substack{n_1, m_1 \\ n_2, m_2}} \Gamma_{n_1 n_2 N}^{m_1 m_2 M} Z_{n_1}^{m_1*}(\mathbf{s}_1) Z_{n_2}^{m_2*}(\mathbf{s}_2) = \pi \int d^2 q e^{-2\pi i \mathbf{q} \cdot (\mathbf{s}_1 + \mathbf{s}_2)} \tilde{Z}_N^{M*}(2\mathbf{q}) = \frac{\pi}{4} Z_N^{M*} \left( \frac{\mathbf{s}_1 + \mathbf{s}_2}{2} \right), \quad |\mathbf{s}_1| \leq 1, \quad |\mathbf{s}_2| \leq 1. \quad (\text{A7})$$

### Appendix B: No turbulence limit.

We calculate the joint probability (43) using (42) in thin crystal approximation and collinear cases.

a. *Thin crystal approximation.*

$$\begin{aligned} P_N^M(z_{N_1}^{M_1}, z_{N_2}^{M_2}) &\propto \left| \int d^2 \rho_1 \int d^2 \rho_2 \tilde{Z}_{N_1}^{M_1*}(\rho_1) \tilde{Z}_{N_2}^{M_2*}(\rho_2) \mathcal{A}_N^M(\rho_1, \rho_2) \right|^2 \\ &= \left| \int d^2 \rho_1 \tilde{Z}_{N_1}^{M_1*}(\rho_1) \int d^2 \rho_2 \tilde{Z}_N^M(\rho_1 + \rho_2) \tilde{Z}_{N_2}^{M_2*}(\rho_2) \right|^2 \\ &= \left| \int d^2 \rho \tilde{Z}_N^M(\rho) \int d^2 \rho_1 \tilde{Z}_{N_1}^{M_1*}(\rho_1) \tilde{Z}_{N_2}^{M_2*}(\rho - \rho_1) \right|^2, \quad (\rho = \rho_1 + \rho_2, \rho_1 = \rho_1) \\ &= \left| \int d^2 \rho \tilde{Z}_N^M(\rho) \left( \tilde{Z}_{N_1}^{M_1*} * \tilde{Z}_{N_2}^{M_2*} \right)(\rho) \right|^2 = \left| \sum_{N_3} A_{N_1 N_2 N_3}^{M_1, M_2, M_1 + M_2} \int d^2 \rho \tilde{Z}_N^M(\rho) \tilde{Z}_{N_3}^{M_1 + M_2*}(\rho) \right|^2 \\ &= \left| \sum_{N_3} A_{N_1 N_2 N_3}^{M_1 M_2, M_1 + M_2} \delta_{N N_3} \delta_{M, M_1 + M_2} \right|^2 = \left| A_{N_1 N_2 N}^{M_1 M_2 M} \right|^2, \end{aligned} \quad (\text{B1})$$

where we used (42) in the first line, and the Fourier transform of (11) in the fourth line.

b.  $\rho_1 = \rho_2 = \rho$  case.

$$P_N^M(z_{N_1}^{M_1}, z_{N_2}^{M_2}) \propto \left| \int d^2 \rho \tilde{Z}_{N_1}^{M_1*}(\rho) \tilde{Z}_{N_2}^{M_2*}(\rho) \mathcal{A}_N^M(\rho, \rho) \right|^2 = \left| \int d^2 \rho \tilde{Z}_{N_1}^{M_1*}(\rho) \tilde{Z}_{N_2}^{M_2*}(\rho) \tilde{Z}_N^M(2\rho) \right|^2 \propto \left| \Gamma_{N_1 N_2 N}^{M_1 M_2 M} \right|^2. \quad (\text{B2})$$

The above results are consistent with Eq. (31) for a single  $Z_N^M$  pump profile.

### Appendix C: Derivation of (46)

a. *Continuous Spatial Representation:* We write the joint probability (43) and consider, for simplicity, the case  $\rho_1 = \rho_2 = \rho$ :

$$\begin{aligned} P_N^M(z_{N_1}^{M_1}, z_{N_2}^{M_2}) &= \frac{k^4}{z^4} \left\langle \left| \int d^2 \rho \tilde{Z}_{N_1}^{M_1*} \left( \frac{kR}{z} \rho \right) \tilde{Z}_{N_2}^{M_2*} \left( \frac{kR}{z} \rho \right) \int d^2 s Z_N^M \left( \frac{\mathbf{s}}{R} \right) e^{2\pi i \frac{2k}{z} \mathbf{s} \cdot \rho} e^{2\psi(\mathbf{s}, \rho)} \right|^2 \right\rangle \\ &= \frac{k^4}{z^4} \iint d^2 \rho_1 d^2 \rho_2 \tilde{Z}_{N_1}^{M_1*} \left( \frac{kR}{z} \rho_1 \right) \tilde{Z}_{N_2}^{M_2*} \left( \frac{kR}{z} \rho_1 \right) \tilde{Z}_{N_1}^{M_1} \left( \frac{kR}{z} \rho_2 \right) \tilde{Z}_{N_2}^{M_2} \left( \frac{kR}{z} \rho_2 \right) \\ &\quad \times \iint d^2 s_1 d^2 s_2 Z_N^M \left( \frac{\mathbf{s}_1}{R} \right) Z_N^{M*} \left( \frac{\mathbf{s}_2}{R} \right) e^{2\pi i \frac{2k}{z} (\mathbf{s}_1 \cdot \rho_1 - \mathbf{s}_2 \cdot \rho_2)} \left\langle e^{2[\psi(\mathbf{s}_1, \rho_1) + \psi^*(\mathbf{s}_2, \rho_2)]} \right\rangle, \end{aligned} \quad (\text{C1})$$

where we also write the various quantities in dimensionless form ( $\rho \rightarrow \frac{kR}{z} \rho$ ,  $\mathbf{s} \rightarrow \frac{\mathbf{s}}{R}$ ). Using the method of cumulants up to second order,  $\langle \exp(\psi) \rangle = \exp(\langle \psi \rangle + \frac{1}{2}(\langle \psi^2 \rangle - \langle \psi \rangle^2))$ , we write  $\langle \exp[2(\psi(\mathbf{s}_1, \rho_1) + \psi^*(\mathbf{s}_2, \rho_2))] \rangle =$

$\exp[-2D(\boldsymbol{\rho}_1 - \boldsymbol{\rho}_2, \mathbf{s}_1 - \mathbf{s}_2)]$ , where [11]  $D(\mathbf{p}, \mathbf{Q}) = \frac{\gamma k}{z}(p^2 + \mathbf{p} \cdot \mathbf{Q} + Q^2)$ , with  $\gamma \equiv 0.4(\sigma_R^2)^{6/5}$ . We now use the identity (15) and simplify the expression of the probability further:

$$P_N^M(z_{N_1}^{M_1}, z_{N_2}^{M_2}) = \frac{k^4}{z^4} 4 \sum_{nm} \Gamma_{N_1 N_2 n}^{M_1 M_2 m*} 4 \sum_{n'm'} \Gamma_{N_1 N_2 n'}^{M_1 M_2 m'} \iint d^2 s_1 d^2 s_2 Z_N^M(\mathbf{s}_1/R) Z_N^{M*}(\mathbf{s}_2/R) \\ \times \iint d^2 \rho_1 d^2 \rho_2 \tilde{Z}_n^{m*} \left( 2 \frac{kR}{z} \boldsymbol{\rho}_1 \right) \tilde{Z}_{n'}^{m'} \left( 2 \frac{kR}{z} \boldsymbol{\rho}_2 \right) e^{2\pi i \frac{2k}{z} (\mathbf{s}_1 \cdot \boldsymbol{\rho}_1 - \mathbf{s}_2 \cdot \boldsymbol{\rho}_2)} e^{-2\frac{\gamma k}{z} [|\mathbf{s}_1 - \mathbf{s}_2|^2 + |\boldsymbol{\rho}_1 - \boldsymbol{\rho}_2|^2 + (\mathbf{s}_1 - \mathbf{s}_2) \cdot (\boldsymbol{\rho}_1 - \boldsymbol{\rho}_2)]}. \quad (\text{C2})$$

Defining  $\mathbf{Q} = \mathbf{s}_1 - \mathbf{s}_2$ ,  $2\mathbf{S} = \mathbf{s}_1 + \mathbf{s}_2$ ,  $\mathbf{p} = \boldsymbol{\rho}_1 - \boldsymbol{\rho}_2$  and  $2\mathbf{P} = \boldsymbol{\rho}_1 + \boldsymbol{\rho}_2$ , such that  $d^2 s_1 d^2 s_2 = d^2 S d^2 Q$  and  $d^2 \rho_1 d^2 \rho_2 = d^2 p d^2 P$ , the probability can be cast into

$$P_N^M(z_{N_1}^{M_1}, z_{N_2}^{M_2}) = \sum_{nn'} \Gamma_{N_1 N_2 n}^{M_1 M_2 m*} \Gamma_{N_1 N_2 n'}^{M_1 M_2 m'} I_{nn'N}^{mm'M}, \quad (\text{C3})$$

where  $m = m' = M_1 + M_2$  due to selection rules imposed by  $\Gamma$ s and

$$I_{nn'N}^{mm'M} = \frac{16k^4}{z^4} \int d^2 p \int d^2 Q \left[ \int d^2 S Z_N^M \left( \frac{1}{R}(\mathbf{S} + \mathbf{Q}/2) \right) Z_N^{M*} \left( \frac{1}{R}(\mathbf{S} - \mathbf{Q}/2) \right) e^{2\pi i \frac{2k}{z} \mathbf{S} \cdot \mathbf{p}} \right] \\ \times e^{-2\frac{\gamma k}{z} [Q^2 + p^2 + \mathbf{Q} \cdot \mathbf{p}]} \left[ \int d^2 P \tilde{Z}_n^{m*} \left( \frac{kR}{z}(2\mathbf{P} + \mathbf{p}) \right) \tilde{Z}_{n'}^{m'} \left( \frac{kR}{z}(2\mathbf{P} - \mathbf{p}) \right) e^{2\pi i \frac{2k}{z} \mathbf{Q} \cdot \mathbf{p}} \right]. \quad (\text{C4})$$

b. *Decoupling via Fourier-Zernike Addition:* The integrals in square brackets (hereafter called  $I_N^M(\mathbf{Q}, \mathbf{p})$  and  $I_{nn'}^{mm'M}(\mathbf{Q}, \mathbf{p})$ , respectively) can be calculated analytically with the help of the addition theorem (13).

$$I_{nn'}^{mm'M}(\mathbf{Q}, \mathbf{p}) = \int d^2 P \tilde{Z}_n^{m*} \left( \frac{kR}{z}(2\mathbf{P} + \mathbf{p}) \right) \tilde{Z}_{n'}^{m'} \left( \frac{kR}{z}(2\mathbf{P} - \mathbf{p}) \right) e^{2\pi i \frac{k}{z} 2\mathbf{Q} \cdot \mathbf{p}}. \quad (\text{C5})$$

Now define  $\mathbf{v} = \frac{kR}{z}\mathbf{p}$ ,  $\mathbf{q} = \frac{kR}{z}(2\mathbf{P} - \mathbf{p})$ , and use the identity (13), then (15).

$$I_{nn'}^{mm'M}(\mathbf{Q}, \mathbf{p}) = \frac{z^2}{4k^2 R^2} \int d^2 q \tilde{Z}_n^{m*}(\mathbf{q} + 2\mathbf{v}) \tilde{Z}_{n'}^{m'}(\mathbf{q}) e^{2\pi i \frac{1}{R} \mathbf{Q} \cdot (\mathbf{q} + \mathbf{v})} \\ = \frac{z^2}{4k^2 R^2 \pi} \sum_{\substack{n_1 n_2 \\ m_1 m_2}} A_{n_1 n_2 n}^{m_1 m_2 m*} \tilde{Z}_{n_2}^{m_2*}(2\mathbf{v}) \int d^2 q \tilde{Z}_{n'}^{m'}(\mathbf{q}) \tilde{Z}_{n_1}^{m_1*}(\mathbf{q}) e^{2\pi i \frac{1}{R} \mathbf{Q} \cdot (\mathbf{q} + \mathbf{v})} \\ = \frac{z^2}{k^2 R^2 \pi} e^{2\pi i \frac{1}{R} \mathbf{Q} \cdot \mathbf{v}} \sum_{\substack{n_1 n_2 \\ m_1 m_2}} A_{n_1 n_2 n}^{m_1 m_2 m*} \tilde{Z}_{n_2}^{m_2*}(2\mathbf{v}) \sum_{n_3 m_3} \Gamma_{n' n_1 n_3}^{m', -m_1 m_3} (-1)^{n_1} \int d^2 q \tilde{Z}_{n_3}^{m_3}(2\mathbf{q}) e^{2\pi i \frac{1}{R} \mathbf{Q} \cdot \mathbf{q}} \\ = \frac{z^2}{4k^2 R^2 \pi} e^{2\pi i \frac{k}{z} \mathbf{Q} \cdot \mathbf{p}} \sum_{\substack{n_1 n_2 \\ m_1 m_2}} A_{n_1 n_2 n}^{m_1 m_2 m*} \tilde{Z}_{n_2}^{m_2*} \left( \frac{2kR}{z} \mathbf{p} \right) \sum_{n_3 m_3} \Gamma_{n' n_1 n_3}^{m', -m_1 m_3} (-1)^{m_3 + n_1} Z_{n_3}^{m_3} \left( \frac{\mathbf{Q}}{2R} \right). \quad (\text{C6})$$

Similarly, we have

$$I_N^M(\mathbf{Q}, \mathbf{p}) = \int d^2 S Z_N^M \left( \frac{1}{R}(\mathbf{S} + \mathbf{Q}/2) \right) Z_N^{M*} \left( \frac{1}{R}(\mathbf{S} - \mathbf{Q}/2) \right) e^{2\pi i \frac{k}{z} 2\mathbf{S} \cdot \mathbf{p}} \\ = \frac{R^2}{\pi} e^{-2\pi i \frac{k}{z} \mathbf{Q} \cdot \mathbf{p}} \sum_{\substack{n_1' n_2' n_3' \\ m_1' m_2' m_3'}} (-1)^{n_1' + m_3'} A_{n_1' n_2' N}^{m_1' m_2' M} \Gamma_{N n_1' n_3'}^{M, -m_1' m_3'} \tilde{Z}_{n_2'}^{m_2'} \left( \frac{2kR}{z} \mathbf{p} \right) Z_{n_3'}^{m_3'} \left( \frac{\mathbf{Q}}{2R} \right). \quad (\text{C7})$$

Finally,

$$I_{nn'N}^{mm'M} = \frac{16k^4}{z^4} \int d^2 p \int d^2 Q e^{-2\frac{\gamma k}{z} [Q^2 + p^2 + \mathbf{Q} \cdot \mathbf{p}]} I_{nn'}^{M_1 M_2}(\mathbf{Q}, \mathbf{p}) I_N^M(\mathbf{Q}, \mathbf{p}) \\ = \frac{4k^2}{\pi^2 z^2} \sum_{\substack{n_1 n_2 n_3 \\ n_1' n_2' n_3' \\ m_1 m_2 m_3 \\ m_1' m_2' m_3'}} (-1)^{n_1' + m_3' + n_1 + m_3} A_{n_1' n_2' N}^{m_1' m_2' M} \Gamma_{N n_1' n_3'}^{M, -m_1' m_3'} A_{n_1 n_2 n}^{m_1 m_2 m*} \Gamma_{n' n_1 n_3}^{m', -m_1 m_3} \\ \times \int d^2 p \int d^2 Q e^{-2\frac{\gamma k}{z} [Q^2 + p^2 + \mathbf{Q} \cdot \mathbf{p}]} \tilde{Z}_{n_2}^{m_2*} \left( \frac{2kR}{z} \mathbf{p} \right) \tilde{Z}_{n_2'}^{m_2'} \left( \frac{2kR}{z} \mathbf{p} \right) Z_{n_3}^{m_3} \left( \frac{\mathbf{Q}}{2R} \right) Z_{n_3'}^{m_3'} \left( \frac{\mathbf{Q}}{2R} \right). \quad (\text{C8})$$

Using again the definitions of  $\Gamma$  and  $A$  to linearize the Zernike products, we get

$$\begin{aligned} \Gamma_{nn'N}^{mm'M} &= \frac{4k^2}{\pi^2 z^2} \sum_{\substack{n_1 n_2 n_3 \\ n'_1 n'_2 n'_3 \\ m_1 m_2 m_3 \\ m'_1 m'_2 m'_3}} (-1)^{n'_1+m'_3+n_1+m_3} A_{n'_1 n'_2 N}^{m'_1 m'_2 M} \Gamma_{N n'_1 n'_3}^{M, -m'_1 m'_3*} A_{n_1 n_2 n}^{m_1 m_2 m*} \Gamma_{n' n_1 n_3}^{m', -m_1 m_3*} \\ &\times 4 \sum_{\substack{n_4 n'_4 \\ m_4 m'_4}} (-1)^{n_2} \Gamma_{n_2 n'_2 n_4}^{-m_2 m'_2 m_4} A_{n_3 n'_3 n'_4}^{m_3, -m'_3 m'_4} \int d^2 p \int d^2 Q e^{-2\frac{\gamma k}{z}[Q^2+p^2+\mathbf{Q}\cdot\mathbf{p}]} \tilde{Z}_{n_4}^{m_4} \left(\frac{4kR}{z}\mathbf{p}\right) Z_{n'_4}^{m'_4} \left(\frac{\mathbf{Q}}{2R}\right). \end{aligned} \quad (\text{C9})$$

To evaluate the last integrals, defined as  $\mathcal{T}_{n_4 n'_4}^{m_4 m'_4}$ , change the variables  $\mathbf{u} = \mathbf{p} + \frac{\mathbf{Q}}{2}$  and use again Eq. (13),

$$\begin{aligned} \mathcal{T}_{n_4 n'_4}^{m_4 m'_4} &\equiv \int d^2 Q e^{-\frac{3\gamma k}{2z}Q^2} Z_{n'_4}^{m'_4} \left(\frac{\mathbf{Q}}{2R}\right) \int d^2 u e^{-2\frac{\gamma k}{z}u^2} \tilde{Z}_{n_4}^{m_4} \left(\frac{4kR}{z}(\mathbf{u} - \mathbf{Q}/2)\right) \\ &= \sum_{\substack{n_5 n'_5 \\ m_5 m'_5}} A_{n_5 n'_5 n_4}^{m_5 m'_5 m_4} \int d^2 Q e^{-\frac{3\gamma k}{2z}Q^2} Z_{n'_4}^{m'_4} \left(\frac{\mathbf{Q}}{2R}\right) \tilde{Z}_{n_5}^{m_5} \left(-\frac{2kR}{z}\mathbf{Q}\right) \int d^2 u e^{-2\frac{\gamma k}{z}u^2} \tilde{Z}_{n'_5}^{m'_5} \left(\frac{4kR}{z}\mathbf{u}\right). \end{aligned} \quad (\text{C10})$$

*c. Evaluation of the Turbulence Tensor:* Define

$$\begin{aligned} G_{n'_5}^{m'_5}(\gamma) &= \int d^2 u e^{-2\frac{\gamma k}{z}u^2} \tilde{Z}_{n'_5}^{m'_5} \left(\frac{4kR}{z}\mathbf{u}\right) = 2\pi \delta_{m'_5 0} i^{n'_5} \sqrt{n'_5 + 1} \frac{z}{4kR} \int_0^\infty du e^{-2\frac{\gamma k}{z}u^2} J_{n'_5+1} \left(\frac{8\pi kR}{z}u\right) \\ &= 2\pi \delta_{m'_5 0} i^{n'_5} \sqrt{n'_5 + 1} \frac{\pi z}{4\gamma k} \left(\sqrt{\frac{8\pi^2 kR^2}{\gamma z}}\right)^{n'_5} \frac{\Gamma\left(\frac{n'_5+2}{2}\right)}{\Gamma(n'_5+2)} {}_1F_1\left(\frac{n'_5+2}{2}; n'_5+2; -\frac{8\pi^2 kR^2}{\gamma z}\right) \end{aligned} \quad (\text{C11})$$

where we used [32, 6.631-1]) and the fact that, for even  $n$ ,  $Z_n^0(0) = \sqrt{n+1}(-1)^{n/2} = \sqrt{n+1}i^n$ , and

$$\mathcal{G}_{n'_4 n'_5}^{m'_4 m'_5}(\gamma) = \int d^2 Q e^{-\frac{3\gamma k}{2z}Q^2} Z_{n'_4}^{m'_4} \left(\frac{\mathbf{Q}}{2R}\right) \tilde{Z}_{n'_5}^{m'_5} \left(-\frac{2kR}{z}\mathbf{Q}\right). \quad (\text{C12})$$

As  $\gamma \rightarrow 0$ ,  ${}_1F_1(a; b; -x) \rightarrow \frac{\Gamma(b)}{\Gamma(b-a)} x^{-a}$ , and  $G_{n'_5}^{m'_5} \rightarrow \frac{z^2}{16k^2 R^2} Z_{n'_5}^{m'_5}(0)$ . The probability (C3) takes the form

$$\begin{aligned} P_N^M(z_{N_1}^{M_1}, z_{N_2}^{M_2}) &= \left(\frac{4k}{\pi z}\right)^2 \sum_{\substack{nn_1 n_2 n_3 n_4 n_5 \\ n' n'_1 n'_2 n'_3 n'_4 n'_5 \\ m_1 m_2 m_3 m_4 m_5 \\ m'_1 m'_2 m'_3 m'_4 m'_5}} (-1)^{n'_1+m'_3+n_1+m_3+n_2} \Gamma_{N_1 N_2 n}^{M_1 M_2 m} A_{n_1 n_2 n}^{m_1 m_2 m*} \Gamma_{N_1 N_2 n'}^{M_1 M_2 m'*} \Gamma_{n' n_1 n_3}^{m', -m_1 m_3*} \\ &\times A_{n_3 n'_3 n'_4}^{m_3, -m'_3 m'_4*} A_{n'_1 n'_2 N}^{m'_1 m'_2 M} \Gamma_{n_2 n'_2 n_4}^{-m_2 m'_2 m_4*} \Gamma_{N n'_1 n'_3}^{M, -m'_1 m'_3} A_{n_5 n'_5 n_4}^{m_5 m'_5 m_4} \mathcal{G}_{n'_4 n'_5}^{m'_4, m'_5}(\gamma) G_{n'_5}^{m'_5}(\gamma) \end{aligned} \quad (\text{C13})$$

Substitute the continuous integral definitions of  $A$  and  $\Gamma$ , and assigning spatial integration variables  $(\mathbf{s}, \mathbf{s}_1, \mathbf{s}_2, \mathbf{s}_3)$  to the four  $A$ -tensors, and frequency integration variables  $(\mathbf{q}, \mathbf{q}_1, \mathbf{q}_2, \mathbf{q}_3, \mathbf{q}_4)$  to the five  $\Gamma$ -tensors. The intermediate

summations naturally group pairs of spatial and Fourier Zernike polynomials sharing identical indices.

$$\begin{aligned}
P_N^M(z_{N_1}^{M_1}, z_{N_2}^{M_2}) &= \left(\frac{4k}{\pi z}\right)^2 \frac{1}{\pi^9} \iiint d^2q d^2q_1 d^2q_2 \iint d^2q_3 d^2q_4 \iiint d^2s d^2s_1 d^2s_2 d^2s_3 \\
&\times \tilde{Z}_{N_1}^{M_1}(\mathbf{q}) \tilde{Z}_{N_2}^{M_2}(\mathbf{q}) \tilde{Z}_{N_1}^{M_1*}(\mathbf{q}_1) \tilde{Z}_{N_2}^{M_2*}(\mathbf{q}_1) \tilde{Z}_N^M(\mathbf{q}_4) Z_N^{M*}(\mathbf{s}_2) \\
&\times \underbrace{\left[ \sum_{nm} Z_n^m(\mathbf{s}) \tilde{Z}_n^{m*}(2\mathbf{q}) \right]}_{\pi e^{-2\pi i \mathbf{s} \cdot 2\mathbf{q}}} \underbrace{\left[ \sum_{n'm'} \tilde{Z}_{n'}^{m'}(2\mathbf{q}_1) \tilde{Z}_{n'}^{m'*}(\mathbf{q}_2) \right]}_{\pi \tilde{Z}_0^0(\mathbf{q}_2 - 2\mathbf{q}_1)} \underbrace{\left[ \sum_{n_1 m_1} (-1)^{n_1} Z_{n_1}^{m_1*}(\mathbf{s}) \tilde{Z}_{n_1}^{-m_1*}(\mathbf{q}_2) \right]}_{\pi e^{2\pi i \mathbf{s} \cdot \mathbf{q}_2}} \\
&\times \underbrace{\left[ \sum_{n_2 m_2} (-1)^{n_2} Z_{n_2}^{m_2*}(\mathbf{s}) \tilde{Z}_{n_2}^{-m_2*}(\mathbf{q}_3) \right]}_{\pi e^{2\pi i \mathbf{s} \cdot \mathbf{q}_3}} \underbrace{\left[ \sum_{n_3 m_3} (-1)^{m_3} Z_{n_3}^{m_3*}(\mathbf{s}_1) \tilde{Z}_{n_3}^{m_3}(2\mathbf{q}_2) \right]}_{\pi e^{-2\pi i \mathbf{s}_1 \cdot 2\mathbf{q}_2}} \underbrace{\left[ \sum_{n'_1 m'_1} (-1)^{n'_1} Z_{n'_1}^{m'_1}(\mathbf{s}_2) \tilde{Z}_{n'_1}^{-m'_1}(\mathbf{q}_4) \right]}_{\pi e^{-2\pi i \mathbf{s}_2 \cdot \mathbf{q}_4}} \\
&\times \underbrace{\left[ \sum_{n'_2 m'_2} Z_{n'_2}^{m'_2}(\mathbf{s}_2) \tilde{Z}_{n'_2}^{m'_2*}(\mathbf{q}_3) \right]}_{\pi e^{-2\pi i \mathbf{s}_2 \cdot \mathbf{q}_3}} \underbrace{\left[ \sum_{n'_3 m'_3} (-1)^{m'_3} Z_{n'_3}^{-m'_3*}(\mathbf{s}_1) \tilde{Z}_{n'_3}^{m'_3*}(2\mathbf{q}_4) \right]}_{\pi e^{2\pi i \mathbf{s}_1 \cdot 2\mathbf{q}_4}} \underbrace{\left[ \sum_{n_4 m_4} Z_{n_4}^{m_4*}(\mathbf{s}_3) \tilde{Z}_{n_4}^{m_4}(2\mathbf{q}_3) \right]}_{\pi e^{2\pi i \mathbf{s}_3 \cdot 2\mathbf{q}_3}} \\
&\times \sum_{\substack{n'_4 n_5 \\ m'_4 m_5}} \mathcal{G}_{n'_4 n_5}^{m'_4, m_5}(\gamma) Z_{n'_4}^{m'_4}(\mathbf{s}_1) Z_{n_5}^{m_5}(\mathbf{s}_3) \sum_{n'_5 m'_5} G_{n'_5}^{m'_5}(\gamma) Z_{n'_5}^{m'_5}(\mathbf{s}_3). \tag{C14}
\end{aligned}$$

Substituting and rearranging, we get

$$\begin{aligned}
P_N^M(z_{N_1}^{M_1}, z_{N_2}^{M_2}) &= \left(\frac{4k}{\pi z}\right)^2 \iiint d^2q d^2q_1 d^2q_3 d^2q_4 \tilde{Z}_{N_1}^{M_1}(\mathbf{q}) \tilde{Z}_{N_2}^{M_2}(\mathbf{q}) \tilde{Z}_{N_1}^{M_1*}(\mathbf{q}_1) \tilde{Z}_{N_2}^{M_2*}(\mathbf{q}_1) \tilde{Z}_N^M(\mathbf{q}_4) \\
&\times \int d^2s_2 e^{-2\pi i \mathbf{s}_2 \cdot (\mathbf{q}_4 + \mathbf{q}_3)} Z_N^{M*}(\mathbf{s}_2) \underbrace{\int d^2s e^{-2\pi i \mathbf{s} \cdot 2\mathbf{q}} e^{2\pi i \mathbf{s} \cdot 2\mathbf{q}_1} e^{2\pi i \mathbf{s} \cdot \mathbf{q}_3}}_{\tilde{Z}_0^0(2\mathbf{q} - 2\mathbf{q}_1 - \mathbf{q}_3)} \sum_{\substack{n'_4 n_5 \\ m'_4 m_5}} \mathcal{G}_{n'_4 n_5}^{m'_4, m_5}(\gamma) \\
&\times \int d^2s_1 e^{2\pi i \mathbf{s}_1 \cdot (2\mathbf{q}_4 - 4\mathbf{q}_1)} Z_{n'_4}^{m'_4}(\mathbf{s}_1) \int d^2s_3 e^{2\pi i \mathbf{s}_3 \cdot 2\mathbf{q}_3} Z_{n_5}^{m_5}(\mathbf{s}_3) \sum_{n'_5 m'_5} G_{n'_5}^{m'_5}(\gamma) Z_{n'_5}^{m'_5}(\mathbf{s}_3) \\
&= \left(\frac{4k}{\pi z}\right)^2 \frac{1}{4} \iiint d^2q_1 d^2q_3 d^2q_4 \tilde{Z}_{N_1}^{M_1}(\mathbf{q}_1 + \mathbf{q}_3/2) \tilde{Z}_{N_2}^{M_2}(\mathbf{q}_1 + \mathbf{q}_3/2) \tilde{Z}_{N_1}^{M_1*}(\mathbf{q}_1) \tilde{Z}_{N_2}^{M_2*}(\mathbf{q}_1) \tilde{Z}_N^M(\mathbf{q}_4) \tilde{Z}_N^{M*}(\mathbf{q}_3 + \mathbf{q}_4) \\
&\times \int_{|\mathbf{Q}| \leq 2R} d^2Q e^{-\frac{3\gamma k}{2z} Q^2} \underbrace{\sum_{n'_4 m'_4} \tilde{Z}_{n'_4}^{m'_4}(2\mathbf{q}_4 - 4\mathbf{q}_1) Z_{n'_4}^{m'_4}\left(\frac{\mathbf{Q}}{2R}\right)}_{\pi e^{2\pi i \left(\frac{1}{2R} \bar{\mathbf{Q}}\right) \cdot (4\mathbf{q}_1 - 2\mathbf{q}_4)}} \\
&\times \int d^2s_3 e^{2\pi i \mathbf{s}_3 \cdot 2\mathbf{q}_3} \sum_{n'_5 m'_5} G_{n'_5}^{m'_5}(\gamma) Z_{n'_5}^{m'_5}(\mathbf{s}_3) \underbrace{\sum_{n_5 m_5} \tilde{Z}_{n_5}^{m_5}\left(-\frac{2kR}{z} \mathbf{Q}\right) Z_{n_5}^{m_5}(\mathbf{s}_3)}_{\pi e^{2\pi i \left(\frac{2kR}{z} \mathbf{Q}\right) \cdot \mathbf{s}_3}} \\
&= \left(\frac{4k}{\pi z}\right)^2 \frac{\pi^2}{4} \iiint d^2q_1 d^2q_3 d^2q_4 \tilde{Z}_{N_1}^{M_1}(\mathbf{q}_1 + \mathbf{q}_3/2) \tilde{Z}_{N_2}^{M_2}(\mathbf{q}_1 + \mathbf{q}_3/2) \tilde{Z}_{N_1}^{M_1*}(\mathbf{q}_1) \tilde{Z}_{N_2}^{M_2*}(\mathbf{q}_1) \tilde{Z}_N^M(\mathbf{q}_4) \tilde{Z}_N^{M*}(\mathbf{q}_3 + \mathbf{q}_4) \\
&\times \int d^2Q Z_0^0\left(\frac{\mathbf{Q}}{2R}\right) e^{-\frac{3\gamma k}{2z} Q^2} e^{2\pi i \left(\frac{1}{2R} \bar{\mathbf{Q}}\right) \cdot (4\mathbf{q}_1 - 2\mathbf{q}_4)} \int d^2s_3 e^{2\pi i \mathbf{s}_3 \cdot 2\mathbf{q}_3} \sum_{n'_5 m'_5} G_{n'_5}^{m'_5}(\gamma) Z_{n'_5}^{m'_5}(\mathbf{s}_3) e^{2\pi i \left(\frac{2kR}{z} \bar{\mathbf{Q}}\right) \cdot \mathbf{s}_3}, \tag{C15}
\end{aligned}$$

where  $\bar{\mathbf{Q}} = (Q, -\phi)$  is the vector  $\mathbf{Q}$  reflected around the x-axis, and we substituted  $\mathcal{G}_{n'_4 n_5}^{m'_4, m_5}$  with (C12).

*d. Final Discrete Tensor Collapse:* In the Fraunhofer regime one can drop the factors  $e^{-\frac{3\gamma k}{2z}Q^2}$  and  $e^{2\pi i(\frac{2kR}{z}\bar{\mathbf{Q}})\cdot\mathbf{s}_3}$  and get

$$\begin{aligned} P_N^M(\tilde{Z}_{N_1}^{M_1}, \tilde{Z}_{N_2}^{M_2}) &= \left(\frac{4kR}{z}\right)^2 \iiint d^2q_1 d^2q_3 d^2q_4 \tilde{Z}_{N_1}^{M_1}(\mathbf{q}_1 + \mathbf{q}_3/2) \tilde{Z}_{N_2}^{M_2}(\mathbf{q}_1 + \mathbf{q}_3/2) \tilde{Z}_{N_1}^{M_1*}(\mathbf{q}_1) \tilde{Z}_{N_2}^{M_2*}(\mathbf{q}_1) \\ &\quad \times \tilde{Z}_N^M(\mathbf{q}_4) \tilde{Z}_N^{M*}(\mathbf{q}_3 + \mathbf{q}_4) \tilde{Z}_0^0(4\mathbf{q}_1 - 2\mathbf{q}_4) \sum_{n'_5 m'_5} G_{n'_5}^{m'_5}(\gamma) \tilde{Z}_{n'_5}^{m'_5}(2\mathbf{q}_3) \\ &= \left(\frac{kR}{4z}\right)^2 \int d^2u \tilde{Z}_{N_1}^{M_1}(\mathbf{u}) \tilde{Z}_{N_2}^{M_2}(\mathbf{u}) \tilde{Z}_N^{M*}(2\mathbf{u}) \int d^2u_1 \tilde{Z}_{N_1}^{M_1*}(\mathbf{u}_1) \tilde{Z}_{N_2}^{M_2*}(\mathbf{u}_1) \tilde{Z}_N^M(2\mathbf{u}_1) \sum_{n'_5 m'_5} G_{n'_5}^{m'_5}(\gamma) \tilde{Z}_{n'_5}^{m'_5}(2(\mathbf{u} - \mathbf{u}_1)) \end{aligned} \quad (\text{C16})$$

Note that the no-turbulence limit recovers the expected result (45) as  $\sum_{n'_5 m'_5} G_{n'_5}^{m'_5}(\gamma) \tilde{Z}_{n'_5}^{m'_5}(2(\mathbf{u} - \mathbf{u}_1)) \rightarrow \sum_{n'_5 m'_5} Z_{n'_5}^{m'_5}(0) \tilde{Z}_{n'_5}^{m'_5}(2(\mathbf{u} - \mathbf{u}_1)) \propto \pi$ . By applying the addition and linearization formulas (13) and (15) the multi-dimensional integrals completely decouple into a discrete structure:

$$P_N^M(z_{N_1}^{M_1}, z_{N_2}^{M_2}) = \frac{1}{2\pi} \left(\frac{4kR}{z}\right)^2 \sum_{\substack{n_1 n_2 n_3 n_4 n_5 \\ m_1 m_2 m_3 m_4 m_5}} G_{n_5}^{m_5}(\gamma) A_{n_1 n_2 n_5}^{m_1 m_2 m_5} (-1)^{n_4 + n_3} \Gamma_{N_1 N_2 n_3}^{M_1 M_2 m_3} \Gamma_{N_1 N_2 n_4}^{M_1 M_2 m_4*} \Gamma_{n_3 N n_1}^{-m_3 M m_1*} \Gamma_{n_4 N n_2}^{-m_4 M - m_2}. \quad (\text{C17})$$

Noting that  $m_1 = -m_2 = M - M_1 - M_2$ ,  $m_5 = 0$ ,  $m_3 = m_4 = M_1 + M_2$ , hence,  $(-1)^{n_4 + n_3} = (-1)^{m_4 + m_3} = 1$  and defining  $F_n = \sum_{n'} \Gamma_{N_1 N_2 n'}^{M_1 M_2 m'}$   $\Gamma_{n' N n}^{-m' M m*}$ , we finally arrive to

$$P_N^M(z_{N_1}^{M_1}, z_{N_2}^{M_2}) = \sum_{n_1 n_2} \left[ \sum_{n_5} G_{n_5}^0(\gamma) A_{n_1 n_2 n_5}^{m_1, -m_1, 0} \right] F_{n_1} F_{n_2}^*. \quad (\text{C18})$$